



OPEN

SUBJECT AREAS:
MEMBRANE PROTEINS
PLANT SCIENCESReceived
15 August 2014Accepted
29 September 2014Published
21 October 2014Correspondence and
requests for materials
should be addressed to
R.K. (kaldenhoff@bio.
tu-darmstadt.de)

A refined model of water and CO₂ membrane diffusion: Effects and contribution of sterols and proteins

Lei Kai & Ralf Kaldenhoff

Department of Biology, Applied Plant Sciences, Technische Universität Darmstadt, Schnittspahnstrasse 10, D-64287 Darmstadt, Germany.

Black lipid bilayers, a general model system for biomembranes were studied for diffusion rates of small molecules such as water or CO₂ using advanced analysis techniques and cell free synthesized proteins. We provide evidence that by simple insertion of proteins or sterols the diffusion rates of water or those of CO₂ decrease. Insertion of cell free synthesized water permeable aquaporins restored water diffusion rates as well as insertion of CO₂-facilitating aquaporins the CO₂ diffusion. Insertion of water or CO₂ impermeable proteins decreased the respective diffusion rates. Therefore, for normal high cellular CO₂ diffusion rates specific aquaporins are mandatory.

Cells of all living organisms are separated from each other and their environment through lipid bilayer biomembranes. These create distinct zones for cell-specific activities. To explain cellular function and interaction with the environment, it is important to understand biomembrane characteristics. Due to the anticipated resemblance to natural membranes, the biophysical and biochemical characteristics of lipid bilayers formed from isolated purified compounds serve as a model system for experiments designed to test assumptions about functional and biophysical characteristics of biomembranes.

However, cell membranes do not completely resemble lipid bilayers¹. Biomembranes are supplemented with integral and associated proteins as well as non-protein molecules, such as sterols². According to the current general view, additional molecules (i.e., channel or pore proteins) do not restrain membrane-diffusion of small molecules because there is enough remaining bilayer surface even if the membrane area contains abundant amounts of protein³. Regarding sterols as biomembrane components, previous studies indicated that they decreased water permeability of lipid bilayer^{4,5}. For the diffusion of CO₂, only few studies reported on the influence of sterols. Due to technical restrictions of the experiments, these results are still under debate^{6,7}. To our knowledge, the effect of proteins or a combination of proteins and sterols on membrane permeability of small molecules such as water or CO₂ has not been reported to date.

Because the lipid bilayer model is so well established, we also chose it to study transport processes of water and CO₂. It is generally accepted that biomembranes are permeable to these small molecules because theoretical models predict that diffusion of small lipophilic molecules like CO₂ are not rate-limited by the lipid bilayer⁸. However, it is also known that the transport of water, which has a high diffusion rate, can be further improved by the presence of aquaporins.

In order to collect data to compare the lipid bilayer model with biomembranes, we studied lipid bilayer membranes in the presence and absence of sterols or membrane proteins. We added purified aquaporin proteins from cell-free synthesis. In this way, aquaporin function in the lipid bilayer under investigation could be studied without unwanted side effects from membrane contamination of cellular systems.

Results

Influence of sterols and proteins on water permeability of lipid bilayer membranes. Water permeability of the membrane lipid bilayer was determined via volume change of liposomes. Liposomes of large unilamellar vesicles were subjected to hyperosmotic conditions, in which the change of volume causes a change in scattered light signal intensity, which was recorded via a stopped-flow spectrophotometer. Two aquaporins, *NtAQP1* and *NtPIP2;1*, were integrated into liposomes, and their influences on water permeability were measured. Fitted light-scattering curves are shown in Figure 1C. In a previous study, *NtAQP1* was demonstrated to be a non-water-

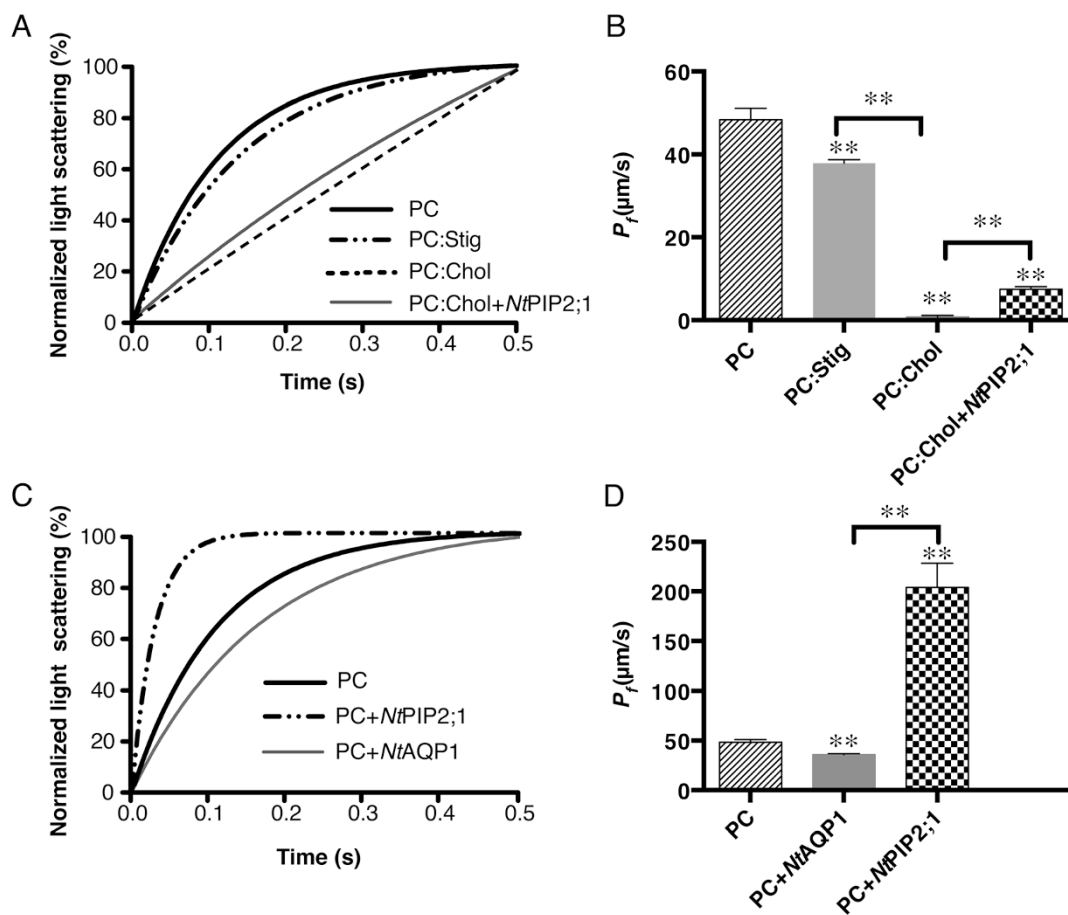


Figure 1 | Comparison of the water permeability of lipid vesicles with aquaporins and/or sterols. Liposomes and proteo-liposomes were measured by stopped-flow light scattering at 10 °C. A 200-mM osmotic gradient was generated by rapidly mixing a vesicle suspension in assay buffer with equal volume of assay buffer plus 400 mM sucrose. An average of 7–12 independent experiments was performed for each sample. The single exponential function was used to fit the light scattering data. (A), average of the fitted curves of the light scattering from empty liposome prepared with PC:Stig (25% molar percentage Stig mixed with PC), PC:Chol (50% molar percentage Chol), and proteo-liposome of *NtPIP2;1* integrated into a PC:Chol-liposome. (B), calculated water permeability coefficient P_f (mean \pm S.D) of samples from A. (C), average of the fitted curves of the light scattering signal from proteo-liposomes with *NtAQP1* or *NtPIP2;1* integrated into a PC-liposome. (D), calculated water permeability coefficient P_f (mean \pm S.D) of samples from (C). See Table S1 for detailed calculations. Significant test of two samples was determined by two-tailed student's t-test, ** right above each column means $P < 0.0001$ if compared to PC.

permeable aquaporin⁹. When inserted into a soybean L- α -phosphatidylcholine (PC)-liposome, the water permeability was reduced to 25%. In contrast, *NtPIP2;1*, characterized as a water channel aquaporin⁹, increased the water permeability of a PC-liposome three fold. The PC was mixed with cholesterol (Chol) and stigmasterol (Stig) to prepare liposomes for forming a mixed lipid bilayer. Light-scattering data were measured in a stopped-flow spectrophotometer. Fitted curves are shown in Figure 1A. Addition of sterols, such as Chol or Stig, reduced water permeability (see Figure 1B and Table S1). In the case of a high molar percentage of Chol (50%), the water permeability was reduced from 48.39 $\mu\text{m/s}$ to 0.79 $\mu\text{m/s}$, corresponding to a reduction of about 60 fold. However, the effect of Stig (25%) was not as pronounced as that of Chol, which reduced the water permeability to about 21%. In addition, PC:Chol-proteoliposomes with *NtPIP2;1* inserted recovered the water permeability by a factor of about 10 compared to empty PC:Chol-liposomes. Nevertheless, the water permeability was still low in comparison to empty PC-liposomes (See Table S1).

Cholesterol altered lipid bilayer water permeability. Results from Figure 1 indicate that Chol had a significant effect on the water permeability of the lipid bilayer. To elucidate the Chol concentration effect, an experiment was performed with liposomes that

had different molar percentages of Chol in PC. Fitted curves of light scattering are presented in Figure 2A; calculated P_f values are summarized in Figure 2B and Table S2. Results from the calculated water permeability showed a negative correlation with the molar concentration of Chol. Using up to 20% Chol, the water permeability declined by about 50%. However, the effect of Chol on water permeability reduction became more distinct when the concentration was greater than 30%. When Chol concentrations reached 50%, which is in a 1:1 molar ratio to PC, the water permeability decreased to 1.5% of the original water permeability (See Table S2 for summary of P_f calculation).

Influence of proteins and sterols on the CO₂ permeability of lipid bilayer membranes. Carbon dioxide flux across the lipid bilayer was measured by applying a micro-pH electrode that continuously recorded voltage while moving toward the lipid bilayer. Its movement was controlled by a micromanipulator. Voltage data was converted to pH values using the calibration function. All pH values for a single measurement were used for plotting curves. The average of 3–5 independent measurements for each type of sample are given in Figures 3A–C. Analogous to the water permeability experiments, two sterols, Chol and Stig, and two different aquaporins, *NtAQP1* and *NtPIP2;1*, were used to study the effects

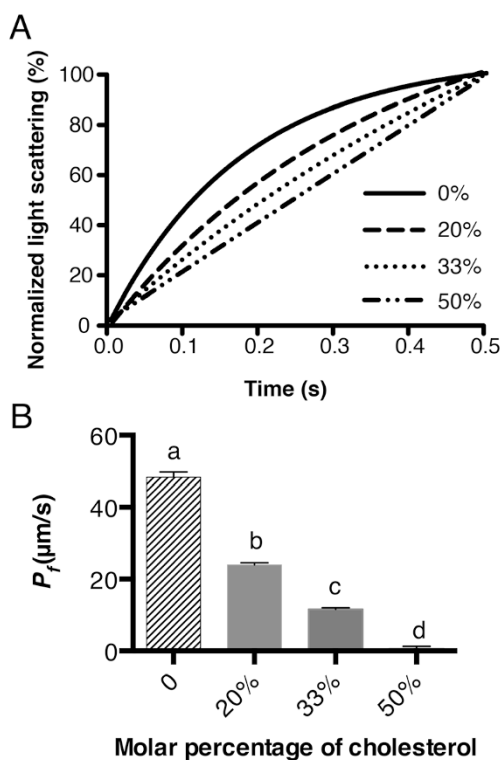


Figure 2 | Effect of Chol concentration on the water permeability of the lipid bilayer. (A), average of the fitted curves of 8–10 independent measurements. (B), calculated P_f (mean \pm SD) value of water permeability of corresponding samples. Letters a, b, c, d are significantly different from each other ($P < 0.0001$), determined by two-tailed student's t-test. See Table S2 for detailed numbers of calculations.

of proteins and sterols on the CO_2 permeability of the membrane lipid bilayer. The CO_2 flux across the membrane lipid bilayer with a diameter 150–200 μm formed in Teflon foil is described by J_{M,CO_2} . Within the distance of 50 μm , a linear fit of the pH as a function of distance from the membrane was used to characterize the change of pH. The slope of the fitted curve was used to calculate J_{M,CO_2} , using equation [6] as depicted in the materials and methods section. As shown in Figure 3D, the insertion of the CO_2 impermeable aquaporin *NtPIP2;1* decreased the J_{M,CO_2} to about 50% compared to PC, while insertion of the CO_2 -permeable aquaporin *NtAQP1* did not increase or decrease J_{M,CO_2} of the PC lipid bilayer. Amounts of 25% Stig and 67% Chol, which were the highest possible molar percentages where lipid bilayers could be formed, were used, and they reduced the CO_2 flux (J_{M,CO_2}) to about 50% and 85%, respectively, compared to that of the PC lipid bilayer (Figure 3D). In the case where both sterols and proteins were inserted into the PC lipid bilayer, *NtAQP1* restored the CO_2 flux of the PC:Stig lipid bilayer to the level of the pure PC lipid bilayer, while insertion of *NtPIP2;1* did not further reduce the CO_2 flux of PC:Stig lipid bilayers.

Cholesterol content altered the CO_2 flux across the membrane lipid bilayers. The Chol was blended with PC to different molar percentages, ranging from 0–67%. A planar membrane was formed with the corresponding lipid mixture. The CO_2 flux across the membrane was then measured using the micro-pH electrode. The profile of pH change caused by the CO_2 diffusion across the membrane is shown in Figure 4A. The calculated J_{M,CO_2} is shown in Figure 4B. The reduction of CO_2 flux decreased linearly with the increase in molar percentage of Chol.

Discussion

The fluid mosaic model proposed by Singer and Nicolson³ provided a basis for the study of membrane structure and dynamics. It is composed of the idea that lipids form a randomly organized fluid, which is a flat, bi-dimensional matrix with membrane proteins inserted. The fact that biological membranes contain a variety of different lipids (i.e., phospholipids, sphingolipids, and sterols) as well as large amounts of different membrane proteins (i.e., channel proteins, transporters, signaling proteins, etc.) extends the Singer-Nicolson concept. It was accepted that Chol increases the rigidity of a lipid bilayer⁹. With respect to water permeability, Finkelstein and Cass described reduced water diffusion rates of thin lipid membranes prepared with phospholipids in 1967⁴. Several other studies also demonstrated reduced water permeability of the lipid bilayer^{10,11} in the presence of Chol. In this study, we could confirm the influence of sterols, especially in the case of Chol, on the water permeability of lipid bilayers represented by liposomes. In addition to sterols, we employed two aquaporins (*NtAQP1* and *NtPIP2;1*) with different functions to study the influence of these membrane proteins on the permeability of lipid bilayers, the former operating as a CO_2 channel and the latter functioning as a water channel^{9,12} in biological systems. Because we have employed pure proteins from a cell-free transcription/translation system, any regulation from a cellular system or activity from components remaining from protein isolation (i.e., other membrane proteins) were very unlikely.

Insertion of the cell-free-synthesized water channel *NtPIP2;1* showed increased water permeability in liposomes consisting of PC or a mixture of PC and Chol. Although a nearly 10-fold increase in water permeability was observed with the insertion of *NtPIP2;1* into the PC:Chol liposome, the water permeability was still relatively low compared to that of the PC liposome. This could indicate the influence of Chol on the function of *NtPIP2;1* through lipid-protein interactions, which corresponds to the conclusion of Tong et al.¹³, who claimed that the activity of AQP0 depends on the lipid bilayer environment of the protein. Insertion of the water-impermeable aquaporin *NtAQP1* slightly decreased the water permeability. This supports the notion that merely the simple insertion or presence of water impermeable membrane proteins could decrease membrane water diffusion.

Unlike water, CO_2 , as a lipophilic gas molecule, was thought to be highly permeable to biological membranes due to its high solubility in lipids. With the finding of CO_2 -tight membranes, such as the apical membranes of epithelial cells¹⁴, and CO_2 -permeable channel proteins^{12,15,16}, the classical concept of a highly CO_2 -permeable biological membrane was challenged. Similar to the experiments designed to study water permeability, we included sterols or sterols together with aquaporins to investigate their influence on the CO_2 flux across the lipid bilayer. To determine CO_2 diffusion, we applied a two-chamber system described by Missner et al.¹⁷ and adapted it as described. Using this technique, the bottleneck for measuring fast kinetics of the CO_2 flux across membranes was circumvented. During a relatively long time period, the CO_2 concentration gradient from one chamber to the other was constant and not limited by CO_2 availability. Thus, the system was time-independent and capable of precisely measuring very high diffusion rates, as those theoretically expected for CO_2 . Sterols, such as Stig or Chol, showed similar effects on reducing CO_2 flux across the membrane, which resemble the effects on water diffusion. Up to 67% Chol reduced the CO_2 flux to only 15% of the original permeability of the PC lipid bilayer. Experiments with a similar intention were performed by Itel et al. using mass spectrometry to determine CO_2 diffusion and a reduction by more than 100 fold was observed⁶. Because the detection principle of the pH electrode applied herein is completely different to the experimental design used by Itel et al., we could explain quantitative differences. As outlined above, measurement in a two-chamber system is independent of time over a relatively large measurement

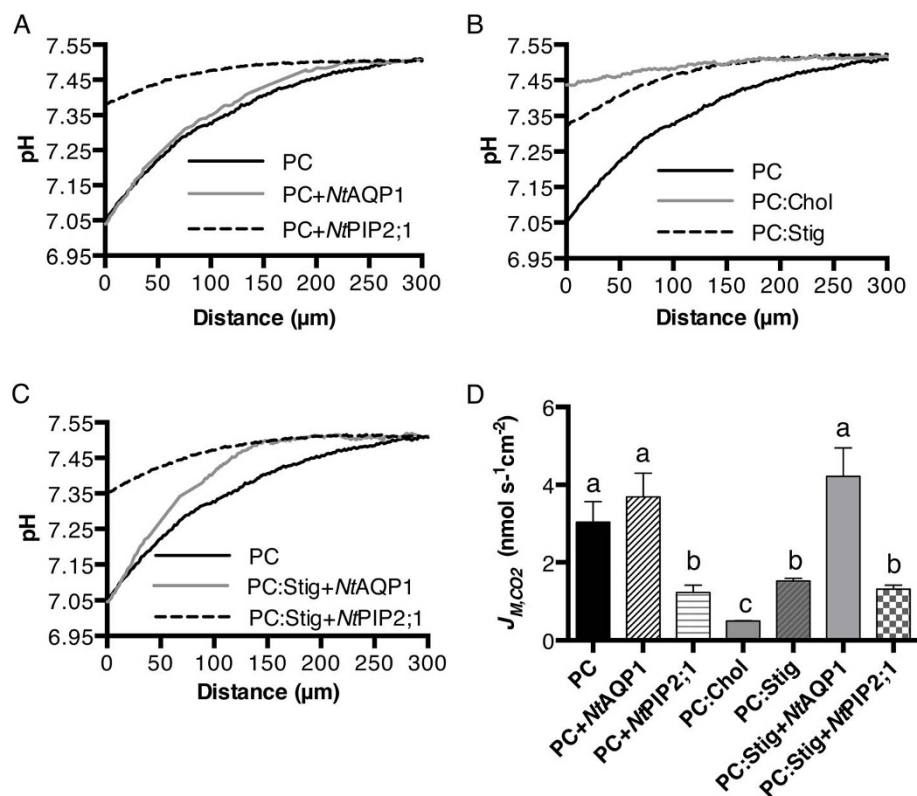


Figure 3 | Comparison of CO₂ fluxes across the lipid bilayer. (A–C), pH profiles in response to CO₂ flux across corresponding lipid bilayers (average of 3–6 curves are shown for each sample) PC:Stig (25% molar percentage Stig mixed with PC) and PC:Chol (67% molar percentage Chol mixed with PC). (D), calculated CO₂ flux across corresponding lipid bilayers from the slope of the pH curve within 50 μ m distance from the formed membrane. The J_{M,CO_2} values are given as means \pm SD ($n = 3-6$). Letters a, b, and c are significantly different from each other ($P < 0.05$), as determined by a two-tailed student's t -test.

period. Therefore, questions concerning technical restrictions that were raised for other reports⁷ can be ruled out. Insertion of the almost CO₂-impermeable aquaporin *NtPIP2;1* reduced the permeability of the PC lipid bilayer by 50%, which could indicate that any CO₂-impermeable protein would have this effect. Insertion of the CO₂-permeable aquaporin *NtAQP1* did not increase the CO₂ flux of the PC lipid bilayer but also did not decrease it like *NtPIP2;1*. This confirms theoretical considerations suggesting that CO₂ diffusion through pure lipid bilayers is so high that CO₂ pores, such as *NtAQP1*, could not increase it further. But these proteins also did not decrease CO₂ diffusion rates.

The CO₂ flux rate was significantly reduced by sterols as well as non-CO₂-conducting aquaporins, such as *NtPIP2;1*. No cumulative effect of CO₂-flux reduction was observed when we introduced both Stig and *NtPIP2;1* together. In case of Stig, restoration of CO₂ diffusion rates were observed with insertion of *NtAQP1*. Since the majority of biological membranes contain proteins and sterols with varying concentrations, the experimental conditions described in this study were closer to conditions in biological membranes than pure black lipid bilayers.

Sterols can reach up to 50% in plasma membranes of eukaryotic cells¹⁸, and even higher local concentrations might exist in lipid rafts¹⁹. In addition, large amounts of membrane proteins could be present in biological membranes. Their weight per membrane area could be as high as that of lipids. Under these circumstances, not only is a protein that facilitates the diffusion of water required for efficient cell metabolism, but also one that facilitates CO₂ diffusion is indispensable.

In conclusion, sterols and non-permeable membrane proteins tend to decrease both water and CO₂ permeability of a lipid bilayer.

Channel proteins for water and CO₂ are mandatory for a high permeability of many biological membranes.

Methods

Expression plasmid construction. The cDNA encoding *NtAQP1* (accession no. AJ001416) and *NtPIP2;1* (accession no. AF440272) from *Nicotiana tabacum* was cloned into the cell-free expression vector pET21a (Merck Bioscience, Darmstadt, Germany) using the constructs previously generated in our lab as templates⁹. The sequence of the primers were as follows:

NtAQP1: AAAAGAATTCATGGCAGAAAACAAAGAAGAAG,

AAAACTCGAGAGACGACTTGTGGAATGG

NtPIP2;1: AAAAGAATTCATGTCAAAGGACGTGATG,

AAAACTCGAGGTTGGTTGGGTTACTCG

Two restriction sites, *EcoRI* and *XhoI* (shown in bold), were used for insertion into the pET21a vector. A poly(His)₆-tag from the vector is expressed together with the native protein for both *NtAQP1* and *NtPIP2;1*.

Protein production. An *Escherichia coli* based cell-free expression system was used for protein expression, as described previously²⁰. The following modifications were made: D-CF (cell-free in presence of detergent) mode expression had a final concentration of 1% (w/v) Brij[®] S20 detergent (Sigma-Aldrich, Taufkirchen, Germany). When the protein was expressed with liposomes, 6 mg/mL final concentration in the reaction mixture was used. A 25-mM amino acid mixture was used to provide enough volume for liposomes. See Supplemental Methods for details and Figure S1 of purification of *NtAQP1* and *NtPIP2;1*.

Liposome preparation. L- α -Phosphatidylcholine from soybean and Chol were purchased from Sigma-Aldrich (Taufkirchen, Germany). Lipid mixtures solubilized in chloroform were first transferred to a round-bottom flask. A thin lipid film was formed by rotary evaporation under controlled vacuum. The flask was then placed in a vacuum chamber overnight. The lipids were reconstituted in 1 mL of assay buffer (50 mM HEPES-KOH, pH 7.5, 50 mM NaCl) to a final concentration of 40 mg/mL by vortexing for 15 min to form multilamellar vesicles. The multilamellar vesicle solution was passed at least 21 times through an Avanti Polar Lipids (Alabaster, Alabama, USA) mini extruder holding a 200-nm Whatman polycarbonate membrane filter (Florham Park, NJ) sandwiched with two filter supports on each side.

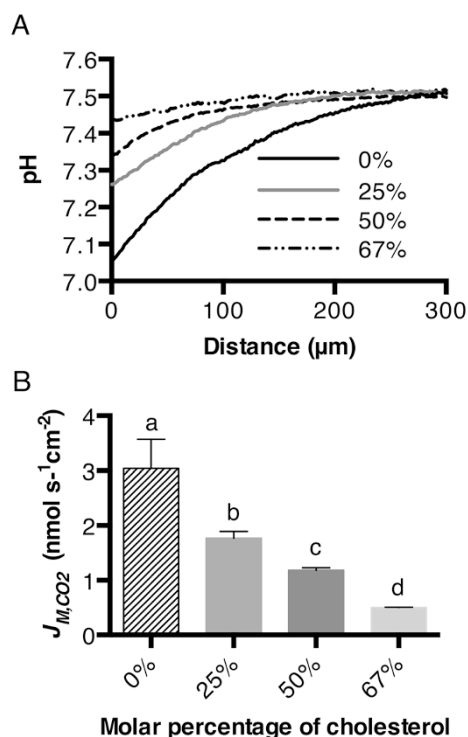


Figure 4 | Effect of Chol concentration on the CO₂ flux across the lipid bilayer. A, pH profiles in response to CO₂ flux across the lipid bilayer with different molar percentages of Chol. B, calculated CO₂ flux across the lipid bilayer with different Chol from the slope of the pH curve within 50 μm distance from the formed membrane. The J_{M,CO_2} values are given as means ± SD (n = 3–6). Letters a, b, c, and d are significantly different from each other ($P < 0.05$), as determined by a two-tailed student's *t*-test.

The resulting unilamellar liposome solution was used for expression or water permeability experiments. See the website of Avanti Polar Lipids for more details.

Sample preparation for water permeability. For water permeability measurements, liposomes were directly added to the mixture with a final concentration around 6 mg/mL. After overnight expression, the reaction mixture was centrifuged at 16,000 g for 30 min. The supernatant was removed, and the pellet was washed three times with an assay buffer. The pellet was then re-suspended with the assay buffer containing TritonX-100 (4-(1,1,3,3-Tetramethylbutyl)phenyl-polyethylene glycol). The suspension was incubated at 30°C with shaking for 2 h. After incubation, the suspension was centrifuged at 16,000 g for 30 min. The supernatant was collected, and bio-beads were added to remove the TritonX-100 to reform the proteo-liposome. The mixture containing bio-beads was incubated at room temperature overnight with gentle shaking. The bio-beads were subsequently removed, and the resulting solution was centrifuged at 500,000 g for 30 min to collect the proteo-liposomes. The proteo-liposome pellet was washed twice with the assay buffer and finally re-suspended in assay buffer with a final liposome concentration of 1 mg/mL. See Supplemental Methods for more details and Figure S2 for protein insertion verification into liposomes.

Water permeability measurements. The water permeability of small, unilamellar liposomes or proteo-liposomes was measured as previously described²⁰. In brief, liposomes or proteo-liposomes were measured at 436 nm in a stopped-flow spectrophotometer (SFM 300, Bio-Logic SAS, Claix, France). Sample suspensions were quickly mixed with equal volumes of a hyperosmotic solution (assay buffer with 400 mM sucrose). Data obtained from the spectrophotometer was fitted into an exponential rise equation; the initial shrinkage rate (*k*) was determined by the fitted curve of 6–10 measurements. The water permeability factor (P_f) of the vesicle samples was calculated using the equation described previously^{20,21}:

$$P_f = \frac{k}{(S/V_0) \times V_w \times \Delta_{osm}} \quad (1)$$

where S/V_0 is the vesicle's initial surface-to-volume ratio, V_w is the partial molar volume of water (18 cm³/mol), and Δ_{osm} is the osmotic driving force. The S/V_0 was calculated by determining the diameters of the proteo-liposomes using dynamic light scattering (ZetaPlus particle sizing software 2.27). The Δ_{osm} was 200 mM in this case.

CO₂ permeability measurements. The basic setup to measure CO₂ permeability of a lipid bilayer was designed according to Missner et al.¹⁷ and further modified by Uehlein et al.²². A scanning pH-sensitive microelectrode, controlled by an IVM-300 electrical micromanipulator (Scientifica, Reutlingen, Germany) with an accuracy of ±0.1 μm, was used to detect the change of pH in solution. The travelling speed of the micromanipulator was controlled via LinLab software provided with the micromanipulator. A two-channel FD223a electrometer (World Precision Instruments, Berlin, Germany) was used to record the voltage signals of the scanning pH electrode. In order to improve the signal-to-noise ratio, an eight-pole BESSEL filter (LHBF-48x [2.1, built 2013], NPI Electronic GmbH, Tamm, Germany) was used. The filtered and amplified signals were recorded by an A/D converter box (USB-6008, National Instruments, Austin [Texas], USA) and analyzed using LabView Signal Express 3.0. See Supplemental Experimental Procedure for micro-pH electrode preparation.

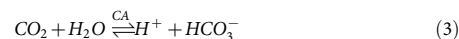
A small hole with a diameter around 150–200 μm was made in Teflon foil by spark induction. The Teflon foil was then fixed between the two chambers sealed with silicon in order to separate the solutions of the two chambers. The only open channel was the 150–200 μm hole in the Teflon ring²². The lipid bilayer was made by the painting method. Successful membrane formation was verified via microscope and resistance measurements. The aquaporin-containing membrane was prepared as described previously: 6 mg lipids or lipid mixture were dissolved in 100 mL n-decane and mixed with an aquaporin fraction (80 μM) at 4°C for 2 h. The mixture was then centrifuged at 16,000 g for 30 min. The upper decane phase was then used for membrane painting.

Analysis of CO₂ flux across the lipid bilayer. According to Fick's first law:

$$J = -D \frac{\partial \phi}{\partial x} \quad (2)$$

In this application, we checked the CO₂ flux across the membrane formed in the middle of the two-chamber system.

Via the activity of carbonic anhydrase, CO₂ molecules were converted instantly into H₂CO₃ when they passed through the membrane. Newly formed H₂CO₃ is a protonated water molecule, resulting in a change of pH.



Since the $[H^+]$ is equal to the $[CO_2]$, the change of CO₂ can be replaced by change of $[H^+]$. Therefore:

$$J_{M,CO_2} = -D_{CO_2} \cdot \frac{\partial [CO_2]}{\partial x} = -D_{CO_2} \cdot \frac{\partial [H^+]}{\partial x} \quad (4)$$

in a buffer solution:

$$\frac{\partial [H^+]}{\partial x} = \beta \cdot \frac{\partial pH}{\partial x} \quad (5)$$

where β is the buffer capacity.

Then,

$$J_{M,CO_2} = D_{CO_2} \cdot \beta \cdot \frac{\partial pH}{\partial x} = D_{CO_2} \cdot \beta \cdot \frac{\partial pH}{\partial x} \quad (6)$$

where the capacity can be calculated via:

$$\beta = 2.303 \cdot \left([H^+] + \frac{C_A K_a [H^+]}{(K_a + [H^+])^2} + [OH^-] \right) \quad (7)$$

The D_{CO_2} was 5.1×10^{-10} m²/s at 25°C and K_a for NaHCO₃ was 6.1. The change of pH as a function of distance away from the membrane was determined via a micro-pH electrode controlled by a micromanipulator, as described previously.

1. Bagatolli, L. A. & Mouritsen, O. G. Is the fluid mosaic (and the accompanying raft hypothesis) a suitable model to describe fundamental features of biological membranes? What may be missing? *Front Plant Sci* **4**, 457 (2013).
2. Nohturfft, A. & Zhang, S. C. Coordination of lipid metabolism in membrane biogenesis. *Annu. Rev. Cell Dev. Biol.* **25**, 539–566 (2009).
3. Singer, S. J. & Nicolson, G. L. The fluid mosaic model of the structure of cell membranes. *Science* **175**, 720–731 (1972).
4. Finkelstein, A. & Cass, A. Effect of cholesterol on the water permeability of thin lipid membranes. *Nature* **216**, 717–718 (1967).
5. Bittman, R. & Blau, L. The phospholipid-cholesterol interaction. Kinetics of water permeability in liposomes. *Biochemistry* **11**, 4831–4839 (1972).
6. Itel, F. *et al.* CO₂ permeability of cell membranes is regulated by membrane cholesterol and protein gas channels. *FASEB journal* **26**, 5182–5191 (2012).
7. Boron, W. F., Endeward, V., Gros, G., Musa-Aziz, R. & Pohl, P. Intrinsic CO₂ permeability of cell membranes and potential biological relevance of CO₂ channels. *Chemphyschem* **12** (2011).
8. Endeward, V., Al-Samir, S., Itel, F. & Gros, G. How does carbon dioxide permeate cell membranes? A discussion of concepts, results and methods. *Front Physiol* **4**, 382 (2014).



9. Otto, B. *et al.* Aquaporin tetramer composition modifies the function of tobacco aquaporins. *J. Biol. Chem.* **285**, 31253–31260 (2010).
10. Saito, H. & Shinoda, W. Cholesterol effect on water permeability through DPPC and PSM lipid bilayers: a molecular dynamics study. *J Phys Chem B* **115** (2011).
11. Michalak, Z., Muzzio, M., Milianta, P. J., Giacomini, R. & Lee, S. Effect of monoglyceride structure and cholesterol content on water permeability of the droplet bilayer. *Langmuir* **29**, 15919–15925 (2013).
12. Uehlein, N., Lovisolo, C., Siefritz, F. & Kaldenhoff, R. The tobacco aquaporin NtAQP1 is a membrane CO₂ pore with physiological functions. *Nature* **425** (2003).
13. Tong, J., Canty, J. T., Briggs, M. M. & McIntosh, T. J. The water permeability of lens aquaporin-0 depends on its lipid bilayer environment. *Exp. Eye Res.* **113**, 32–40, doi:10.1016/j.exer.2013.04.022 (2013).
14. Waisbren, S. J., Geibel, J. P., Modlin, I. M. & Boron, W. F. Unusual permeability properties of gastric gland cells. *Nature* **368**, 332–335 (1994).
15. Nakhoul, N. L., Davis, B. A., Romero, M. F. & Boron, W. F. Effect of expressing the water channel aquaporin-1 on the CO₂ permeability of *Xenopus* oocytes. *Am. J. Physiol.* **274**, C543–548 (1998).
16. Forster, R. E., Gros, G., Lin, L., Ono, Y. & Wunder, M. The effect of 4,4'-diisothiocyanato-stilbene-2,2'-disulfonate on CO₂ permeability of the red blood cell membrane. *Proc. Natl. Acad. Sci. U.S.A.* **95**, 15815–15820 (1998).
17. Missner, A. *et al.* Carbon dioxide transport through membranes. *J. Biol. Chem.* **283**, 25340–25347 (2008).
18. van Meer, G., Voelker, D. R. & Feigenson, G. W. Membrane lipids: where they are and how they behave. *Nat Rev Mol Cell Bio* **9**, 112–124 (2008).
19. Simons, K. & van Meer, G. Lipid sorting in epithelial cells. *Biochemistry* **27**, 6197–6202 (1988).
20. Kai, L. *et al.* Preparative scale production of functional mouse aquaporin 4 using different cell-free expression modes. *PLoS One* **5**, e12972 (2010).
21. Borgnia, M. J., Kozono, D., Calamita, G., Maloney, P. C. & Agre, P. Functional reconstitution and characterization of AqpZ, the *E. coli* water channel protein. *J. Mol. Biol.* **291**, 1169–1179 (1999).
22. Uehlein, N. *et al.* Gas-tight triblock-copolymer membranes are converted to CO₂ permeable by insertion of plant aquaporins. *Sci Rep* **2**, 538 (2012).

Acknowledgments

We would like to thank Dr. Frank Bernhard from Goethe University Frankfurt for the help with regard to cell-free expression techniques. We are grateful to Prof. David T. Hanson from biology department at University of New Mexico for discussion and revision of the manuscript. This work is supported by Deutsche Forschungsgemeinschaft grant (to R. K.).

Author contributions

R.K. and L.K. designed the research and wrote the paper. L.K. performed all the experiments.

Additional information

Supplementary information accompanies this paper at <http://www.nature.com/scientificreports>

Competing financial interests: The authors declare no competing financial interests.

How to cite this article: Kai, L. & Kaldenhoff, R. A refined model of water and CO₂ membrane diffusion: Effects and contribution of sterols and proteins. *Sci. Rep.* **4**, 6665; DOI:10.1038/srep06665 (2014).



This work is licensed under a Creative Commons Attribution-NonCommercial-ShareAlike 4.0 International License. The images or other third party material in this article are included in the article's Creative Commons license, unless indicated otherwise in the credit line; if the material is not included under the Creative Commons license, users will need to obtain permission from the license holder in order to reproduce the material. To view a copy of this license, visit <http://creativecommons.org/licenses/by-nc-sa/4.0/>